

Coding Ants: Using Ant Colony Optimization to Accelerate CT Reconstruction

Eric Papenhausen, Ziyi Zheng and Klaus Mueller

Abstract—There is no one size fits all solution when it comes to CT reconstruction. Many different CT reconstruction algorithms and implementations have been devised in an attempt to solve the problem of producing an image under a specific set of constraints. One optimal CT reconstruction implementation can look very different from another optimal implementation; depending on the data, quality, and time constraints. In this paper, we present a framework that is able to dynamically create and compile new implementations that optimize the multiple objectives contained in CT reconstruction. We then show the results of this framework when applied to a GPU accelerated version of the FDK back-projection algorithm.

Index Terms—CT reconstruction, GPU, ant colony optimization, Filtered backprojection

I. INTRODUCTION

Any CT reconstruction algorithm can be identified as a multi-objective optimization problem. The optimal result will provide the highest quality reconstruction in the shortest time. Many algorithms have been developed and extended, and good parameter settings have been identified to solve this problem under specific conditions [1][4][7]. However, if the boundary conditions change (i.e. noisier projections, different numbers of projections, stricter time constraint, anatomy and pathology, etc.), the existing implementation is rendered sub-optimal, and in some cases, useless.

In this paper, we use swarm optimization to determine an optimal CT reconstruction implementation for any given set of parameters. More specifically, we use the ant colony optimization algorithm to find an optimal implementation of a GPU accelerated FDK back-projection, described in [5].

In this paper, we begin in Section II by discussing related work. Section III gives a brief description of the ant colony system optimization algorithm. Section IV presents the details of the coding ants framework. Section V gives a brief description of the graphics hardware used in our experiments and the structure of a CUDA program. Section VI presents the results of our experiments. Section VII presents future work and Section VIII concludes the paper.

II. RELATED WORK

Recent work has focused on finding good algorithmic parameters for iterative CT reconstruction [9]. Parameter tuning is critical in finding a good balance between image quality and reconstruction speed. The use of GPUs in accelerating CT reconstruction has also become very popular in decreasing reconstruction time [5][8][10]. However, not all GPUs are created equally; and there are many parameters to consider when creating a GPU accelerated program.

Whereas [9] focused on tuning algorithmic parameters, we focus on tuning system level parameters. Our optimizations come from creating a framework that will find an optimal implementation by directly manipulating source code. The optimal implementation may change across different machines and this framework will be able to produce a machine dependent optimal implementation without direct programmer intervention.

III. ANT COLONY SYSTEM

The ant colony system optimization algorithm is a part of the family of swarm optimization algorithms. It is a modification of the ant system algorithm which was designed to mimic the way ants find the shortest path from the ant nest to a food source. Initially ants will choose paths randomly. Once an ant finds food, it will travel back to the nest and emit pheromones so other ants can follow that path to the food source. As other ants follow the pheromone trail, they emit pheromones as well which reinforces the trail. After some time, however, the pheromone trail will evaporate. Given multiple paths to a food source, the pheromones on the shortest path will have the least amount of time to evaporate before being reinforced by another ant. Over time, the ants will converge to the shortest path.

The ant colony system was presented in [2] and was applied to the traveling salesman problem. It modifies the ant system algorithm [3] in several ways to lead to a faster convergence rate. After an ant crosses an edge, the pheromone value of that edge is decayed according to equation 1:

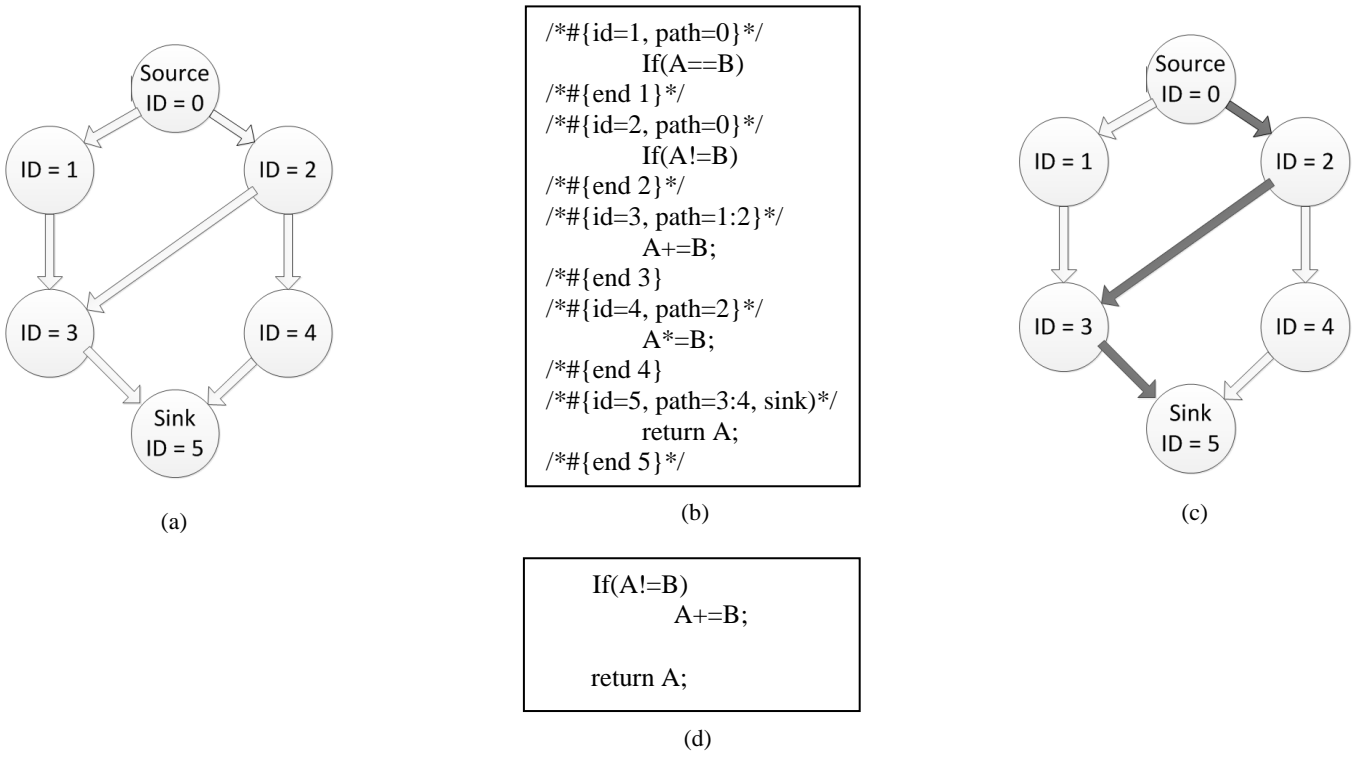


Figure 1. An illustration of the framework presented in this paper. (a) a graph representing all possible implementations of a program. (b) the super source file represented by the graph in (a). (c) a path is selected through the graph. (d) source code corresponding to the path selected in (c).

$$\tau_{ij} = 1 - \varphi \cdot \tau_{ij} + \varphi \cdot \tau_0 \quad (1)$$

where τ_{ij} denotes the pheromone quantity on the edge from state i to state j . The pheromone decay coefficient, φ , determines how much pheromone is decayed after an ant chooses the edge from i to j . The initial pheromone value, τ_0 , is the value every edge has at the beginning of the program. Equation 1 reduces the probability of multiple ants choosing the same path.

After all ants have chosen a path, the pheromone of each edge is updated as follows:

$$\tau_{ij} = 1 - \rho \cdot \tau_{ij} + \rho \cdot \Delta\tau_{ij}^{best} \quad (2)$$

The variable τ_{ij} has the same meaning as equation 1. The variable $\Delta\tau_{ij}^{best}$ evaluates to the inverse of the length of the best path if the edge from i to j was taken by the ant with the best path; otherwise it evaluates to zero. The variable ρ represents the evaporation rate. This leads to a pheromone increase on the edges taken by the ant that produced the best solution; while decaying the pheromones on all other edges. When transitioning from one state to another, the edge is selected probabilistically according to the following probability:

$$p_{ij}^k = \frac{\tau_{ij}^\alpha \eta_{ij}^\beta}{\sum \tau_{ij}^\alpha \eta_{ij}^\beta} \quad (3)$$

where τ_{ij} determines the amount of pheromone on the edge from i to j , and η_{ij} defines some predetermined desirability of that edge (e.g. the inverse of the edge weight). The variables α and β are weighting factors for τ_{ij} and η_{ij} respective-

ly. The variable p_{ij}^k is the probability that an ant will select an edge that goes from state i to state j during the k^{th} iteration.

IV. IMPLEMENTATION

We use the ant colony system described in the previous section to find and create an optimal implementation for a specific set of constraints. In order to do so we define the structure of a program as a directed graph with a single source, at which every ant will start, and a single sink, where every ant will finish. The nodes of the graph correspond to source code snippets. A path from source to sink corresponds to a candidate implementation that can be compiled and executed. The output of the candidate implementation can then be measured and ranked among the other candidate implementations to find the ant with the shortest path for that iteration. The shortest path can be defined as a function of image quality and reconstruction time.

The graph is constructed by creating a super source file. This super source file contains annotated sections of code. These annotations specify node id and incoming edges. Figure 1(a) and 1(b) show the graph and its corresponding super source file. Figure 1(c) and 1(d) show a potential path through the graph, and the corresponding candidate implementation. This super source file is then submitted as input to our program, which converts it to its graph representation and runs the ant colony system algorithm to produce an optimal implementation.

One aspect of our program differs from the traditional ant colony system algorithm. There is no predetermined desirability, η . There is no way of determining edge weight

before running the algorithm. We can still apply the ant colony system algorithm by only considering the pheromone value, τ , when looking at an edge. This is equivalent to setting η to one, for all edges. Equation 4 shows how edges are selected by ants. Our experiments indicate that this still converges to an optimal solution.

$$p_{ij}^k = \frac{\tau_{ij}^\alpha}{\sum \tau_{ij}^\alpha} \quad (4)$$

Since graphics hardware plays such a prominent role in CT reconstruction, our framework provides the option of expanding the graph provided in the super source file to account for different grid and thread block sizes. This is done by copying the code snippets that contain the threads unique ID and offsetting the ID by the grid dimension. This allows the framework to implicitly increase the workload for each thread. Figure 2 shows an example of this. The grid and thread block dimensions determine the granularity of each thread. The smaller the grid and block size, the more work each thread will perform.

```
int tid = blockIdx.x * blockDim.x + threadIdx.x;
    .
    <code>
    .
F_L[tid] = result;
```

(a)

```
int tid = blockIdx.x * blockDim.x + threadIdx.x;
    .
    <code>
    .
F_L[tid] = result;
    .
    <code>
    .
F_L[(blockIdx.x + 8) * blockDim.x + threadIdx.x] = result;
```

(b)

Figure 2. Sample code demonstrating how thread granularity can be increased implicitly. (a) Source code representing a thread granularity of one (e.g. grid = 16, thread block = 16). (b) Source code representing a thread granularity of two (e.g. grid = 8, thread block = 16).

In this specific example a thread in Figure 2b computes two final results and stores them into the respective target locations in memory.

V. GRAPHICS HARDWARE

Modern GPUs follow a “Single Instruction Multiple Thread” (SIMT) model of parallel execution. In this model of execution, every thread executes the same instruction, but over different data. The implementation we attempt to optimize in our experiments use a C-like API called CUDA (Compute Unified Device Architecture) to program NVIDIA GPUs.

The GPU used in our experiments was the NVIDIA GeForce GTX 480. This graphics card contains 15 streaming multiprocessors. Each streaming multiprocessor contains 32 cores. Theoretical computing power of this graphics card is 1.3 TFLOPS. Like all NVIDIA graphics cards, this card has

both on-chip and off-chip memory. Off-chip memory includes global, texture, and constant memory and typically incurs a latency of 400 to 600 clock cycles. On-chip memory includes shared memory as well as cache for texture and constant memory and is much faster than off-chip memory. The GTX 480 has a peak memory bandwidth of 177.4 GB/s for its 1.5 GB DDR5 device memory.

When accessing global memory, it is critical to performance that the access is coalesced. A coalesced memory access will allow multiple memory addresses to be returned with a single memory access; increasing memory bandwidth. A coalesced memory access typically requires every thread in a warp to access consecutive memory addresses. This constraint is relaxed, however, in devices with compute capability of 1.2 and higher. As long as the memory access of each thread is within a 32, 64, or 128 byte segment, depending on the data type, a coalesced memory access is performed.

GPU accelerated applications have a large number of parameters that can be tuned for optimal performance. Occupancy, thread granularity, and memory bandwidth are all examples of the types of parameters that can have a large impact on performance. Tuning one parameter too much can often lead to a sudden decrease in performance in some other aspect of the application. This is what is known as a performance cliff.

VI. EXPERIMENT AND RESULTS

We used the framework presented in this paper to create an optimal GPU accelerated implementation of the FDK back-projection algorithm described in [4]. This back-projection implementation is then tested with the help of the RabbitCT framework [6]. We chose to compose the graph out of the three major implementations presented in [5]. An ant’s path from the source to the sink represents either the first, second, or third configuration presented in [5], or some combination of the three. In this graph we also added a fourth configuration in which two projections are loaded per kernel call.

We ran our framework with 30 ants for 5 iterations. Our super source file described a graph that contained 25 nodes. This graph, however, is replicated for 16 different grid and thread block dimensions; creating a graph that contains 400 nodes. Table 1 shows a comparison of the timings of the FDK implementations that were produced through our framework with the results presented in [5] which were obtained by manually optimizing the code. For the 256³ implementation we found a faster implementation. This configuration loads two projections per kernel invocation and has a thread granularity of two in the x direction. For the 512³ implementation, our framework produced the same code as in [5]. Figure 3 shows a slice of the reconstructed volume. The quality of the reconstruction for the implementations produced by this framework was the same as the quality produced in [5].

TABLE I
RUNTIMES OF BEST KNOWN AND FRAMEWORK PRODUCED
IMPLEMENTATIONS

Configuration	Volume	Time (s)
Framework	256 ³	2.54
Best Known	256 ³	2.71
Framework	512 ³	6.07
Best Known	512 ³	6.07



Figure 3. Slice of the reconstructed image.

The run time of our framework is dependent on the scale of the application it is trying to produce. For each ant, source code is generated, compiled, and executed. For the experiments that we ran, it took approximately 2 hours for all 30 ants to complete 5 iterations. The graph could have been pruned, however, by eliminating nodes that correlate to configurations that we know have bad performance. In our experiments, we included the naïve configuration explained in [5], as a possible implementation. By pruning the graph of bad implementations, we could reduce the number of ants; thus greatly reducing the amount of time required by our framework.

We wish to add that the code produced by the ant colony optimization can be re-used for any new CT reconstruction task with the same boundary conditions the code was generated for. Therefore the optimization overhead is well amortized.

VII. FUTURE WORK

One direction of future work for this framework is to develop a visual interface that is much more user friendly. At its current state, this framework requires the input to be an annotated source file. As the size of this source file grows, it can become difficult to keep track of the graph structure. In the future, we would like to develop a visual interface that clearly shows the graph. Nodes can be easily added or removed from this graph. Source code can be easily added or modified inside a node; and the information that is currently stored in the annotations can be abstracted away.

Another direction of future work, involves using this framework to build an all-encompassing CT reconstruction builder. This would incorporate different CT reconstruction algorithms and implementations. Given a set of parameters,

this CT reconstruction builder would produce an optimal implementation.

VIII. CONCLUSION

In this paper we presented a novel framework for producing an optimal code structure using an ant colony optimization algorithm. Through our experiments in applying our framework to the RabbitCT platform, we have discovered a better implementation for the 256³ volume reconstruction, while producing the same results as [5] for the 512³ implementation.

Although we apply this framework to GPU accelerated CT reconstruction, it is in no way restricted to that field of study. The graph structure that the framework works off of ensures that this framework can be applied to produce an optimal implementation of any type of application.

REFERENCES

- [1] A. Andersen and A. Kak, "Simultaneous algebraic reconstruction technique (SART): A superior implementation of the ART algorithm," *Ultrason. Imaging*, 6:81–94, 1984
- [2] M. Dorigo and L. M. Gambardella. "Ant Colony System: A cooperative learning approach to the traveling salesman problem." *IEEE Transactions on Evolutionary Computation*, 1(1):53–66,
- [3] M. Dorigo, V. Maniezzo, and A. Colomi. "Ant System: Optimization by a colony of cooperating agents." *IEEE Transactions on Systems, Man, and Cybernetics – Part B*, 26(1):29–41, 1996.
- [4] L. Feldkamp, L. Davis, and J. Kress, "Practical cone-beam algorithm," *J. Opt. Soc. Am. Vol 1, No. A6*, 612–619, 1984
- [5] E. Papenhausen, Z. Zheng, and K. Mueller, "GPU-Accelerated Back-Projecting Revisited: Squeezing Performance by Careful Tuning," *Fully Three-Dimensional Image Reconstruction in Radiology and Nuclear Medicine (Potsdam, Germany, 2011)*
- [6] C. Rohkohl, B. Keck, H. G. Hofmann and J. Hornegger, "RabbitCT--an open platform for benchmarking 3D cone-beam reconstruction algorithms," *Medical Physics*, 36:3940, 2009.
- [7] L. Shepp and Y. Vardi, "Maximum likelihood reconstruction for emission tomography," *IEEE Trans. Med. Imag.*, 1(2):113–122, 1982.
- [8] H. Scherl, B. Keck, M. Kowarschik, J. Hornegger, "Fast GPU-based CT reconstruction using the Common Unified Device Architecture (CUDA)," *IEEE Medical Imaging Conference*, 6: 4464-4466, Honolulu, HI, 2007.
- [9] W. Xu, K. Mueller "Learning Effective Parameter Settings for Iterative CT Reconstruction Algorithms," *Fully 3D Image Reconstruction in Radiology and Nuclear Medicine (Beijing, China, 2009)*
- [10] Z. Zheng, K. Mueller "Cache-Aware GPU Memory Scheduling Scheme for CT Back-Projection," *IEEE Medical Imaging Conference*, Oct. 2010.